Physics with muon and hadron beams at COMPASS

R. Geyer
on behalf of the COMPASS collaboration [a*],

[a]Faculty of Physics, Ludwig-Maximilians-University Munich,
Schellingstrasse 4, 80799 Munich

COMPASS is a multi-purpose fixed target experiment at CERN's Super Proton Synchrotron, dedicated to the study of the structure of the nucleon and the spectroscopy of hadrons. The large acceptance and high resolution two stage spectrometer takes advantage of the availability of a variety of high intensity beams (muons and hadrons) with momenta up to 300 GeV/c. During the years 2002-2004 and 2006-2007 high statistics data for inclusive and semi-inclusive deep inelastic scattering were collected using polarized 160 GeV/c muons on ${}^6LiD$ and NH_3 targets. These measurements have produced a wealth of results on the spin structure of the nucleon, both in the longitudinal and in the transverse nucleon spin configuration. Since 2008, COMPASS has focused on the search for exotic hadronic states in central production or diffractive projectile excitation of 190 GeV hadrons on a liquid hydrogen target. Masses up to about 2.5 GeV/c^2 are accessible. An overview on the results obtained so far and a short summary of the future plans of the collaboration will be given.

1. Introduction

The COMPASS (COmmon Muon and Proton Apparatus for Structure and Spectroscopy) experiment at CERN became operational in 2002. Until 2007, the main interest of the collaboration was focused on DIS measurements with 160 GeV μ^+-beams on polarized solid targets in order to study the spin structure of the nucleon. Longitudinally and transversely polarized Deuterons (${}^6LiD$, 2002-2006) and Protons (NH_3, 2007) were used as target materials. More than 2000 Terabyte of data were recorded which corresponds to about $5 \cdot 10^{10}$ events. A variety of results has been meanwhile obtained covering subjects like the polarized structure function g_1 and its first moment [1–3], the gluon polarization inside the nucleon [4,10], production of vector mesons [5], transverse spin effects [6–8] or polarization of hyperons. Only a few days of effective data taking was dedicated in 2004 for hadron beams, when a short pilot run was carried out with 190 GeV negative pions on nuclear targets. Despite the shortness of this run, COMPASS collected a data sample with sufficiently large statistics to be competitive with earlier experiments. First results were obtained in the diffractive excitation of pions via the reaction $\pi^- p \to \pi^-\pi^+\pi^- p$. In 2008 and 2009, COMPASS dedicated its beam time completely for hadron spectroscopy in diffractive scattering and central production. π, K and p with 190 GeV were used as beam particles on LH_2 and nuclear targets. In the following, I will summarize the present situation of the spin structure of the nucleon and present preliminary COMPASS results on the gluon polarization $\Delta G/G$. In the second part, I will report on the meson spectroscopy results obtained from the 2004 pilot run in $\pi^- p \to \pi^-\pi^+\pi^- p$. An outlook on future measurements of COMPASS will be given. COMPASS results on flavor separation of the structure functions, Λ-polarizations, Primakoff measurements and transverse spin effects will be presented by colleagues in the same conference.

2. Spectrometer

The COMPASS physics program mentioned above puts high demands both on the beam and on the experimental setup. The Super Proton Synchrotron (SPS) at CERN delivers proton

*Present address: Reiner Geyer, CERN, 1211 Geneve 23, Switzerland. Reiner.Geyer@cern.ch.

beams, secondary hadron beams (π, K) and tertiary polarized muon beams with momenta between 100 and 300 GeV/c at intensities up to $4 \cdot 10^7 particles/s$, as required by the small cross sections of the processes under investigation in the two experimental programs. COMPASS has been designed to be a versatile apparatus with large acceptance for charged and neutral particles (both in angle and momentum) and particle ID. The apparatus consists of a two stage spectrometer with bending powers of 1 and 4.4 Tm, respectively. Each magnet is preceded and followed by tracking devices. Both stages are completed by electromagnetic and hadronic calorimetry and muon identification. The identification of charged particles takes place in a RICH (Ring Imaging CHerenkov) detector. The target material for DIS measurements is contained in two cells of 60 cm length which are polarized by dynamic nuclear polarization in opposite directions. This allows for the recording with both spin directions simultaneously. Since 2006, a new target solenoid has been used increasing the acceptance from 70 $mrad$ to 180 $mrad$. Also the number of target cells with opposite polarization was increased from 2 (+, -) to 3 (+, -, +). In this configuration the difference of acceptances between the cells with opposite polarizations is significantly reduced. The part upstream of the target consists of a set of detectors which measure direction and momentum of incoming beam particles. A full description of the COMPASS spectrometer can be found under [9]. Modification of the apparatus related to hadron data taking will be described later.

3. The Spin Structure of the Nucleon

Taking into account quark and gluon orbital angular momenta, the nucleon spin projection (in units of $\hbar$) can be written as:

$$\frac{1}{2} = \frac{1}{2}\Delta\Sigma + \Delta G + \Delta L_q + \Delta L_g, \quad (1)$$

where $\Delta\Sigma = \Delta u + \Delta d + \Delta s$ is the first moment of the sum of the quark helicity distributions, ΔG is the first moment of the polarized gluon distribution and L_q and L_g are possible contributions from the orbital momentum from quarks and gluons. The quantities Δq are defined as:

$$\Delta q = \int_0^1 \Delta q(x) dx \quad (2)$$

with

$$\Delta q(x) = (q(x)^{\uparrow\downarrow} + \overline{q}(x)^{\uparrow\downarrow}) - (q(x)^{\uparrow\uparrow} + \overline{q}(x)^{\uparrow\uparrow}) \quad (3)$$

$\Delta q(x)$ can be interpreted as the difference of number densities of quarks and anti-quarks with the flavor $q = u, d, s$ and a momentum fraction x of the nucleon, which have a spin parallel $\uparrow\uparrow$ or anti-parallel $\uparrow\downarrow$ to the nucleon. Experimentally $\Delta\Sigma$ is accessible via the spin dependent structure function $g_1(x) = 1/2 \sum e_q^2 \Delta q(x)$ and using the values of the baryon decay constants $(F+D)$ and $(3F-D)$. g_1 itself can be extracted from the cross section asymmetry of polarized photon nucleon scattering:

$$\frac{g_1(x)}{F_1(x)} \approx \frac{\sigma_{1/2}(x) - \sigma_{3/2}(x)}{\sigma_{1/2}(x) + \sigma_{3/2}(x)} = A_1 \quad (4)$$

$\sigma_{3/2}(x)$ and $\sigma_{1/2}(x)$ are the inclusive cross sections for photon absorption with spin parallel or anti-parallel to the nucleon spin and $F_1(x) = 1/2 \sum e_q^2 q(x)$ is the spin independent structure function. In COMPASS where $g_1(x)$ is extracted from polarized muons (virtual polarized photon scattering) the relation has to be slightly modified to:

$$g_1 \approx \frac{A_\parallel}{D} \cdot \frac{F_2(x)}{2x(1+R)} \quad (5)$$

Here, $A_\parallel$ is the longitudinal cross section asymmetry for polarized muon nucleon scattering. D is the depolarization factor, which takes into account the polarization transfer of virtual photons. $R = \sigma_L/\sigma_T$ is the ratio of the longitudinal and transverse photoabsorption cross sections. First measurements of $\Delta\Sigma$ twenty years ago by the European Muon Collaboration [11,12] resulted in very small values ($\Delta\Sigma = 0.12 \pm 0.17$) - a clear sign that the nucleon spin cannot be carried alone by the spin of the quarks. Later measurements related to g_1, which were performed at DESY,

SLAC, J-Lab and at CERN increased the precision of $\Delta\Sigma$ by more than one order in magnitude and qualitatively confirmed the first result from EMC. An illustration for the improved situation is given in figure 1. Here new results from COMPASS, obtained from the scattering of polarized muons on polarized deuterons, are shown together with those of other experiments for the spinstructure function $g_1^d(x)$ of the deuteron [2,3]. The measured values of COMPASS have been evolved to a common $Q^2 = 3\ (GeV/c)^2$ by a new NLO QCD fit of the world g_1-data, and the first moment Γ_1^N has been evaluated [2]:

$$\Gamma_1^N(Q^2 = 3(GeV/c)^2) = \int_0^1 g_1^N(x)dx = 0.050 \pm 0.003(stat) \pm 0.003(evol) \pm 0.005(syst) \quad (6)$$

(For clarity we use here g_1^N instead of g_1^d, because the correction of the D-wave state of the deuteron has been applied). As a result from the same fit the following value for the quark polarization $\Delta\Sigma$ is obtained as [2]:

$$\Delta\Sigma = 0.30 \pm 0.01(stat) \pm 0.02(evol) \quad (7)$$

Adding the COMPASS results to the world data reduces the error of $\Delta\Sigma$ roughly by a factor of two, mainly owing to the possibility to access small values in x. The original finding of EMC that the spin structure of the nucleon cannot be described alone by the spin of its quark content still persists 20 years later. Consequently the gluon polarization and/or the orbital angular momenta of quarks and gluons must contribute to the spin of the nucleon.

4. Direct Measurements of the Gluon Polarization

One possibility to probe directly the gluon polarization is given by Photon Gluon Fusion (PGF). In COMPASS, PGF events are tagged using either the production of open charm or looking for two-jet events (events with hadron pairs with large transverse momenta p_T). It is important to note that the spin dependence of the basic process of PGF can be calculated in LO by perturbative QCD. The open charm production is

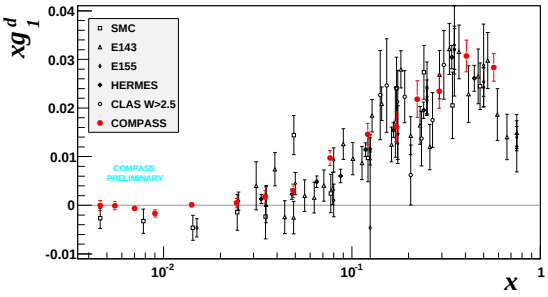

Figure 1. The spin structure function g_1^d as a function of x in comparison with the results of other experiments (SMC, E143, E155, Hermes, Clas). The COMPASS data reduces the experimental uncertainties especially at small x.

regarded to be the cleanest way to probe PGF events, since there are hardly any background processes to be considered. Unfortunately the cross sections are small and large statistics are difficult to be achieved. In first order, the cross-section helicity asymmetry $A_{\parallel}^{c\bar{c}}$ for open charm can be written as:

$$A_{\parallel}^{c\bar{c}} = ((\sigma^{\uparrow\downarrow} - \sigma^{\uparrow\uparrow}))/((\sigma^{\uparrow\downarrow} + \sigma^{\uparrow\uparrow})) \approx a_{LL}^{PGF} \cdot \frac{\Delta g}{g} \quad (8)$$

The arrows indicate the relative beam and target spin orientations. Here a_{LL}^{PGF} is the analyzing power of the underlying process $\mu g \to \mu' c\bar{c}$ which includes also the depolarization factor D. As already mentioned the PGF process can be calculated in LO QCD and thus allows for the determination of a_{LL}^{PGF} from theory. In COMPASS, open charm events are identified by the measurement of the decay of D^0,$\overline{D}^0$,D^{*+} and D^{*-} mesons. Only one meson is required by the event selection. This meson is selected through its decay in one of the two channels: $D^{*+}(2010) \to D^0\pi^+_{slow} \to K^-\pi^+\pi^+_{slow}$ (D^*-sample) and $D^0 \to K^-\pi^+$ (D^0-sample) and their charge conjugates. Meanwhile the full data set from 2002 to 2006 is analyzed. The invariant mass spectra for the D^* and D^0-samples are shown in figure 2. About 8700 events of the first and 37400 events of the second sample were collected.

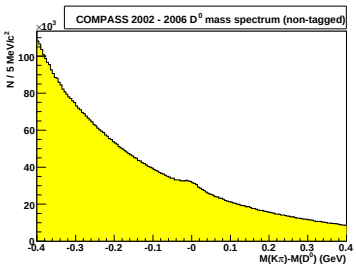

(a) D^0 decaying in $K + \pi$

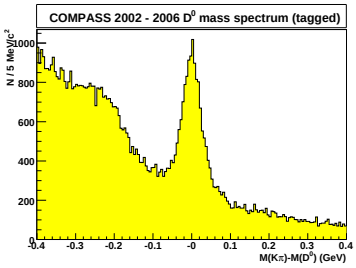

(b) D^* decaying in $K + \pi + \pi_{soft}$

Figure 2. Invariant mass distributions of the $K\pi$-pairs for the D^0 sample with 37398 good events (upper plot) and the D^* sample (lower plot) with 8675 good events [10].

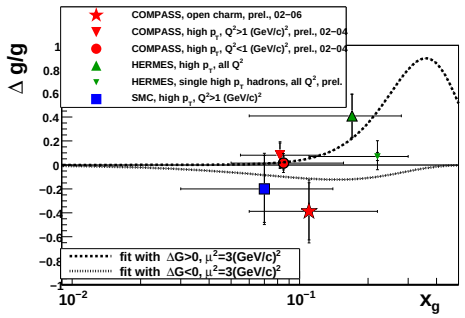

Figure 3. Compilation of the $\langle \Delta g/g \rangle_x$ measurements from open charm and high-p_T hadron pair production by COMPASS [4], SMC [13] and HERMES [14] as a function of x. The horizontal bars mark the range in x for each measurement, the vertical ones give the statistical precision and the total errors (if available). The open charm measurement is at a scale of about 13 $(GeV/c)^2$, other measurements at 3 $(GeV/c)^2$. The curves display two parameterizations from the COMPASS QCD analysis at NLO [2], with $\Delta G > 0$ (broken line) and with $\Delta G < 0$ (dotted line).

The preliminary present value for the gluon polarization of COMPASS is:

$$\langle \frac{\Delta g}{g} \rangle_x = -0.39 \pm 0.24(stat) \pm 0.11(syst) \qquad (9)$$

Here, events with $D^{*+}(2010) \rightarrow D^0\pi^+_{slow} \rightarrow K^-\pi^+\pi^0\pi^+_{slow} + c.c.$ decays were included in the analysis; x is in the range of $0.06 < x < 0.22$ with $\langle x \rangle \approx 0.11$ and a scale $\langle \mu^2 \rangle \approx 13(GeV/c)^2$.

The production of hadron pairs with large transverse momenta p_T is also suited to tag for PGF events. They are produced with much larger statistics. Nevertheless other production mechanisms like DIS and QCD Compton Scattering lead to the same indistinguishable final states and have to be taken into account in the analysis. As a result, the cross-section helicity asymmetry $A_\parallel^{q\bar{q}}$ for high p_T hadron pair production contains in addition to the contribution from PGF a contribution from some background processes A_{bckgrd}.

$$A_\parallel^{q\bar{q}} \approx a_{LL}^{PGF} \cdot \frac{\Delta g}{g} + A_{bckgrd} \qquad (10)$$

A_{bckgrd} has to be determined from simulation calculations using Monte Carlo techniques and thus increases the model dependence in the evaluation of $\langle \frac{\Delta g}{g} \rangle_x$. COMPASS has extracted two values for $\langle \frac{\Delta g}{g} \rangle_x$ from high p_T hadron pair events for two different kinematical regions with $Q^2 > 1$ and $Q^2 < 1$, taking into account different theoretical uncertainties. The preliminary results are: $0.08 \pm 0.10(stat) \pm 0.05(syst)$ and $0.016 \pm 0.058(stat) \pm 0.055(syst)$, respectively. In both analyses, the mean value of $\langle x \rangle \approx 0.085$ and the scale $\langle \mu^2 \rangle \approx 3(GeVc)^2$.

The results are summarized in figure 3 and indicate small values for $\Delta g/g$ around $x \approx 0.1$. Small values are in agreement with values obtained by BNL and Hermes. This can be taken as a hint for a small value for the first moment of the gluon helicity distribution ΔG , although the data points are not sufficient for a prove. Nevertheless the data may be used to constrain the values of $\Delta g(x)$ in future global NLO QCD analysis.

5. Meson Spectroscopy

The simple $SU(3)_{flavor}$ constituent quark model provides an amazingly successful description of the spectrum of light mesons in terms of bound states of quarks q with antiquarks $\overline{q}$ with the flavors u, d or s. The states are grouped into multiplets with the quantum numbers J^{PC}, where J is the total angular momentum, P is the parity and C is the conjugation parity. In addition the isospin I and the G-parity are used to characterize these mesons. In the constituent quark model, the parity quantum numbers of mesons can be related to the angular momentum L and the total spin $S = 0, 1$ of the $q\overline{q}$-pairs: $(P) = -1^{L+1}$, $C = (-1)^{L+S}$, $G = (-1)^{I+L+S}$. Despite the success of the constituent quark model to describe to a large extent the observed meson spectrum, color singlet states in QCD can not only be obtained by $q\overline{q}$ constituent quark pairs, but also in other combinations between quarks, antiquarks and gluons. Such states, like tetra-quark objects ($q\overline{q}q\overline{q}$), Glueballs ($gg$) or hybrids ($q\overline{q}g$) have frequently been predicted by theory but never unambiguously experimentally proven. One complication originates from the fact that these non-$q\overline{q}$-configurations may mix with the ordinary states and are thus, depending on their production rate and the width of the state, difficult to be identified. The observation of states with exotic quantum numbers, which are not accessible in the simple constituent quark model ($J^PC = 0^{--}$, 0^{+-}, 1^{-+}, ...) would give clear evidence for the existence of quark-gluon configurations beyond the constituent quark model, as allowed by QCD.

The hybrid with the lowest mass is predicted in some models to have the quantum numbers $J^{PC} = 1^{-+}$ and thus will not mix with ordinary mesons [15]. Its mass should be in the range between $1.3 - 2.2\ GeV/c^2$. Three experimental candidates were reported for such a state, the $\pi_1(1400)$ seen by E852 [16], VES [17] and Crystal Barrel [18,19], the $\pi_1(1600)$ seen by E852 and VES [20–26,28] and the $\pi_1(2000)$ [25,28]. The resonant nature of these states, however, is still heavily disputed in the community [17,26]. One possibility at COMPASS to search for the production of exotic mesons is diffractive dissociation. Diffractive dissociation is a reaction of the type $a + b \to c + d$, where a is the incoming beam particle, b the target, c is a via Reggeon or Pomeron exchange diffractively produced object and d is the target recoil particle. The production kinematics is described by $t' = |t| - |t_{min}|$, where $t = (p_a - p_c)^2$ is the square of the four momentum transferred from the incoming beam to the outgoing system c and $|t_{min}|$ is the minimum value of $|t|$ which is required for the production of a mass m_c. COMPASS can cover t values ranging from zero up to a few $(GeV/c)^2$. During the Hadron Pilot Run in 2004 of only a few days of effective data taking, COMPASS collected a sufficiently large statistics in order to shed new light on the existence of the $\pi_1(1600)$. A 190 GeV/c π^--beam was used on a $3mm$ lead target. The trigger was based on a multiplicity increase of charged particles after the target, which allowed selecting events of the type $\pi^- p \to \pi^-\pi^+\pi^- p$ (which corresponds to the diffractive process $a + b \to c + d$ with the subsequent decay $c \to \pi^-\pi^+\pi^-$). For the further analysis only events were used, where t' is in the range of $0.1\ (GeV/c)^2 < t' < 1\ (GeV/c)^2$. Figure 4 shows the invariant mass spectrum between 0.5 and 2.5 GeV/c^2 of the corresponding events. The well known resonances $a_1(1260)$, $a_2(1320)$ and $\pi_2(1670)$ are clearly visible in the $\pi^-\pi^+\pi^-$ invariant mass spectrum of 420000 events.

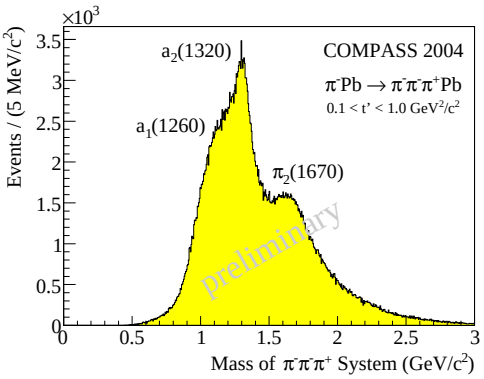

Figure 4. Invariant mass of the $\pi^-\pi^+\pi^-$-system for $0.1 GeV^2/c^2 < t_0 < 1.0\ GeV^2/c^2$.

A partial wave analysis (PWA) of this data set

was performed which is based of the phenomenological isobar model, in which all multiple particle states can be described by sequential two-body decays into intermediate resonances (isobars). For the $\pi^-\pi^+\pi^-$-states, the excited state is thus assumed to decay into a single bachelor pion and a di-pion resonance, which by itself decays again into $\pi^+\pi^-$. All known isovector and isoscalar ($\pi\pi$) resonances have been included into the analysis. In total 42 partial waves are considered by the PWA. The waves are characterized by a set of quantum numbers $J^{PC}M^{\epsilon}[isobar]L$. Here, M is the absolute value of the spin projection of the total angular momentum J of the 3 pion system onto the z-axis (of the Gottfried Jackson frame); ϵ is the reflectivity which describes the symmetry under a reflection through the production plane [29]. L is the orbital angular momentum between the isobar and the bachelor pion.

The PWA is done in two steps. First, a fit of the probability density in 3π phase space is performed in 40 MeV/c^2 bins of the 3π invariant mass m_c. No dependence of the production strength for a given wave on m_c is introduced at this point (mass-independent fit). In the second step a mass-dependent χ^2 fit to the result of the first step is carried out taking into account the mass dependence of the produced resonances through relativistic Breit-Wigner functions (and a possible coherent background). In this second fit only a subset of six waves of the first step were taken into account, selected by their significance or by a rapid phase change in the 1.7 GeV/c^2 mass region. These are: $0^{-+}0^+f_0(980)\pi S$, $1^{++}0^+\rho\pi S$, $2^{-+}0^+f_2(980)\pi S$, $2^{++}1^+\rho\pi D$, $4^{++}1^+\rho\pi G$ and the exotic $1^{-+}1^+\rho\pi P$. The preliminary results obtained for the mass independent and mass dependent fit for the three most prominent contributing waves are shown in figure 5 a-c. Figure 5 d shows the intensity of the exotic wave $1^{-+}1^+\rho\pi P$. In addition to the Breit-Wigner resonance at 1.66 GeV/c^2, which is represented by the line to the right and can be interpreted as the $\pi_1(1600)$, the 1^{-+} wave has a shoulder at lower masses (left line). This shoulder is described in our PWA by a non-resonant background, possibly caused by a Deck-like effect [27]. The resonant

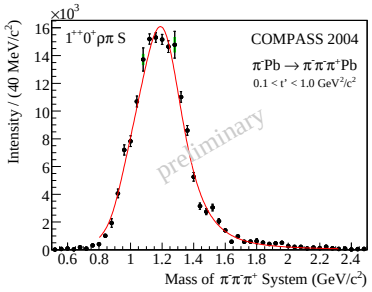

(a) $a_1(1260)$

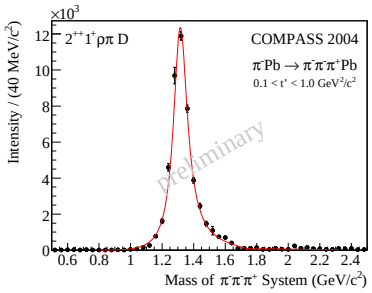

(b) $a_2(1320)$

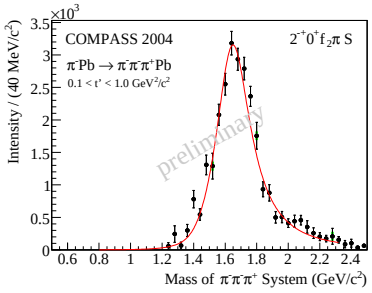

(c) $\pi_2(1670)$

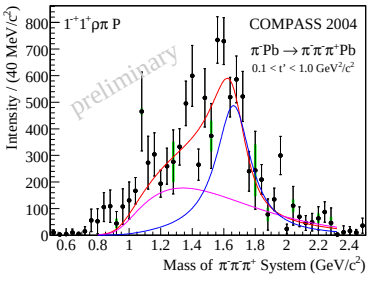

(d) $\pi_1(1600)$

Figure 5. Intensities of major waves $1^{++}0^+\rho\pi S$ (a), $2^{++}1^+\rho\pi D$ (c), and $2^{-+}0^+f_2\pi S$ (b) as well as the intensity of the exotic wave $1^{-+}1^+\rho\pi P$ (d). The lines represent the result of the mass-dependent fit (see text). The results are preliminary.

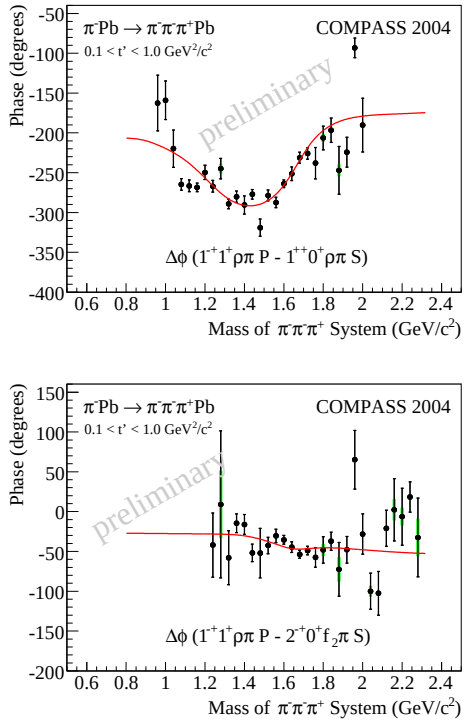

Figure 6. Phase differences of the exotic $1^{-+}1^{+}\rho\pi P$ wave to other resonances seem to confirm its resonant nature (preliminary results). Top: Phase difference between the $1^{-+}1^{+}\rho\pi P$ and the $1^{++}0^{+}\rho\pi S$ wave. Bottom: Phase difference between the $1^{-+}1^{+}\rho\pi P$ and the $2^{-+}0^{+}f_2\pi S$ wave.

nature of the $1^{-+}1^{+}\rho\pi P$ wave can be reconfirmed by the motion of its phase relative to other states. Figure 6 b shows the phase difference between $2^{-+}0^{+}f_2(980)\pi S$ and the exotic wave. No significant change is observed which can be attributed to the fact that both resonances $\pi_1(1600)$ and $\pi_2(1670)$ have similar masses and widths, causing the relative phase to be almost constant. In contrary as shown by figure 6 a, the phase difference relative to the $1^{++}0^{+}\rho\pi S$ state clearly shows variations around 1.6 GeV/c^2. Since the a_1 (1260) is no longer resonating at this mass, both observations can be regarded as an independent verification of the resonant origin of the $\pi_1(1600)$. Nevertheless it is important to note that a reconfirmation of the existence of that resonance by different final states would be essential.

6. Hadron Spectroscopy in 2008 and 2009 at COMPASS

A number of new detectors have been installed in order to optimize the setup. This includes two CEDAR detectors in the beam line to identify beam pions or kaons via Cherenkov radiation, a recoil proton detector consisting of two concentric rings of scintillators surrounding a 40 cm long liquid hydrogen target, a set of silicon microstrip detectors cooled to cryogenic temperatures for improved radiation hardness, five novel GEM detectors with pixel readout for very small area tracking, and 800 radiation-hard Shashlik blocks for the central part of the second electromagnetic calorimeter. The measurements in 2008 were dedicated to the continuation of meson spectroscopy in diffractive scattering with negative pions on protons from a LH_2-target. We expect to increase the presently available world statistics for $\pi_1(1600)$ by about a factor of ten. Since these were the first measurements with hadron beams and a completed electromagnetic calorimetry at COMPASS, final states with π^0 and η have now become accessible to the offline analysis and will lead to new results in different final states. The CEDAR detectors allow now for the measurement of diffractive excitations of K-mesons, which are part of the beam and were measured parasitically. In 2009 COMPASS has mainly been running with 190 GeV/c proton beams. The main goal is the search for neutral exotic mesons in central production, a process where particles will be produced in Reggeon-Reggeon collisions, while the beam and target particles will only loose a small fraction of their energy. Masses up to 2.7 GeV/c^2 are accessible. One of the interesting objects to be studied might be the $f_0(1500) \to \eta\eta$, a state which has been seen by Crystal Barrel and the WA102 collaboration and is often referred to as a glueball candidate with the non exotic quantum numbers 0^{++}. Therefore it can mix with other isoscalar mesons. Also here COMPASS has the chance to improve the world statistics in central production by a factor of 10 and put new insights

to the origin of this resonance. The meson spectrum in the mass region up to 2.5 GeV/c^2 will be explored with high statistics for the first time.

7. Outlook and Future Perspectives

Just recently COMPASS was approved for two years of additional data taking using the muon beam and the polarized proton target. The beam time will be evenly split on both, precision measurements of the transverse spin effects in SIDIS and precision measurements of the spin-dependent longitudinal structure function of the proton at small x. The years after will be based on a new proposal which is presently under preparation. One major part of the new proposal will be the study of the nucleon structure via Generalized Parton Distributions by measuring Deeply Virtual Compton Scattering (DVCS) and Deeply Virtual Meson Production (DVPM) on both an unpolarized liquid hydrogen and a polarized target. A second part will focus on the study of transverse momentum dependent and transversity distributions in Drell-Yan by detecting the Drell-Yan process in the scattering of a pion beam on a transversely polarized target. The continuation of measurements with hadron beams is also planned.

REFERENCES

1. COMPASS Collaboration, E.S. Ageev, et al., Phys. Lett. B 612 (2005) 154.
2. COMPASS Collaboration, V.Yu. Alexakhin, et al., Phys. Lett. B 647 (2007) 8.
3. COMPASS Collaboration, V.Yu. Alexakhin, et al., Phys. Lett. B 647 (2007) 330.
4. COMPASS Collaboration, E.S. Ageev, et al., Phys. Lett. B 633 (2006) 25.
5. COMPASS Collaboration, M. Alekseev, et al., Eur. Phys. J. C 52, 255-265 (2007).
6. COMPASS Collaboration, V.Yu. Alexakhin, et al., Phys. Rev. Lett. 94, 202002 (2005).
7. COMPASS Collaboration, E.S. Ageev, et al., Nucl. Phys. B 765 (2007) 31-70.
8. COMPASS Collaboration, M. Alekseev, et al., Phys. Lett. B 673 (2009) 127-135.
9. COMPASS Collaboration, P. Abbon, et al., Nucl. Instrum. Methods A 577 (2007) 455.
10. COMPASS Collaboration, M. Alekseev, et al., Phys. Lett. B 676 (2009) 31.
11. EMC Collaboration, J. Ashman, et al., Nucl. Phys. B 328 (1989) 1.
12. EMC Collaboration, J. Ashman, et al., Phys. Lett. B 206 (1988) 364.
13. SMC Collaboration, B. Adeva, et al., Phys. Rev. D 70 (2004) 012002.
14. HERMES Collaboration, A. Airapetian, et al., Phys. Rev. Lett. 84 (2000) 2584.
15. K. J. Juge, J. Kuti, and C. Morningstar, AIP Conf. Proc. 688, 193 (2004).
16. D. R. Thompson et al., Phys. Rev. Lett. 79, 1630 (1997).
17. V. Dorofeev et al., AIP Conf. Proc. 619, 143 (2002).
18. A. Abele et al., Phys. Lett. B423, 175 (1998).
19. A. Abele et al., Phys. Lett. B446, 349 (1999).
20. G. S. Adams et al., Phys. Rev. Lett. 81, 5760 (1998).
21. S. U. Chung et al., Phys. Rev. D65, 072001 (2002).
22. Y. Khokhlov, Nucl. Phys. A663, 596 (2000).
23. G. M. Beladidze et al., Phys. Lett. B313, 276 (1993).
24. E. I. Ivanov et al., Phys. Rev. Lett. 86, 3977 (2001).
25. J. Kuhn et al., Phys. Lett. B595, 109 (2004).
26. D. V. Amelin et al., Phys. Atom. Nucl. 68, 359 (2005).
27. R. T. Deck, Phys. Rev. Lett. 13, 169 (1964).
28. M. Lu et al., Phys. Rev. Lett. 94, 032002 (2005).
29. S. U. Chung and T. L. Trueman, Phys. Rev. D11, 633 (1975).